

PAPER

Embedding monomers and dimers of sulfonamide antibiotics into high silica zeolite Y: an experimental and computational study of the tautomeric forms involved†

Cite this: *RSC Advances*, 2013, 3, 7427

Ilaria Braschi,^{*ab} Geo Paul,^b Giorgio Gatti,^b Maurizio Cossi^{*b} and Leonardo Marchese^b

This work is a second step towards the systematic study of the embedding of sulfonamide antibiotics into a synthetic high silica zeolite Y (HSZ-Y) with hydrophobic properties. In the previous paper [Braschi *et al.*, *Langmuir* 2010, **31**, 9524], the irreversible adsorption from water into HSZ-Y of three sulfonamides was studied by enlightening the host–guest interactions and, in the case of the smallest sized sulfadiazine, the guest–guest interactions of dimeric species inside the zeolite cage. Here the HSZ-Y was loaded with six sulfonamides, namely: sulfanilamide, sulfapyridine, sulfathiazole, sulfadimethoxine, sulfadoxine and sulfamerazine. With the exception of sulfanilamide, which showed scarce affinity for HSZ-Y (maximum loading 3% zeolite dry weight), the other sulfa drugs adsorbed at ca. 28% zeolite dry weight on average, and this is relevant for both water depollution and drug delivery issues. The low affinity of sulfanilamide for HSZ-Y was ascribed to its high hydrophilicity (water solubility 15–40 times higher than other drugs). The most stable tautomeric (amide or imide) form of each antibiotic adsorbed in zeolite Y was proposed by means of IR and solid state NMR spectroscopy augmented by computational modelling. The small dimensions and favourable stabilization energy allow the embedding of imidic and amidic dimers of sulfathiazole and sulfapyridine, respectively, inside the zeolite cage whereas the remaining sulfa drugs adsorbed in monomeric amidic forms.

Received 25th September 2012,
Accepted 28th February 2013

DOI: 10.1039/c3ra22290j

www.rsc.org/advances

1. Introduction

Since their discovery in the 1930s, up to now sulfonamide antibiotics (sulfa drugs) have been used for their broad spectrum of activities against bacterial, protozoal and fungal infections in human therapy, livestock production and aquaculture.^{1–3} Sulfonamides represent in Europe the third most commercialized antibiotic class for veterinary application.³ The administration of doses that are higher than needed and the failure to respect a proper withdrawal period before butchering can result in the occurrence of unwanted residues in edible products.^{4,5} The persistence of sulfa drugs is not limited to foodstuffs, but it is also a concern in soil compartments, owing to the spreading of manure contaminated by antibiotics.

Sulfonamides are formed by an aniline ring attached by C4 to the sulphur atom of a sulfonamide moiety (–SO₂–NH–). The

sulfonamide nitrogen atom can be differently substituted with a hydrogen atom (sulfanilamide, see Table 1) or with an aromatic heterocycle ring. In some *pro*-drugs, the sulfonamide nitrogen atom forms an azo group (–N=N–) which is usually hydrolysed *in situ* to sulfanilamide. The acidic nature of the sulfonamide moiety⁶ makes these drugs partially anionic at the pH values of agricultural soils and natural or artificial water bodies. In the anionic form, sulfonamides are scarcely adsorbed and slightly degraded in the soil system.^{7,8} As a consequence of their persistence, sulfonamides can exert a high level of bacterial resistance.^{9,10}

Despite the need to find affordable sorbents to clean-up water bodies polluted with sulfonamides, only a methodology based on high silica zeolite Y (HSZ-Y) has been proposed.^{11–13} HSZ-Y with a 200 SiO₂/Al₂O₃ molar ratio ensures a fast and irreversible removal of sulfadiazine, sulfamethazine and sulfachloropyridazine from water¹² thanks to the occurrence of multiple interactions (namely van der Waals and weak H-bonding) between zeolite cages and sulfonamides.¹³ The maximum amount of sulfonamide adsorbed by HSZ-Y is around 20% zeolite dry weight (DW).¹² This amount is high enough to consider this material not only affordable for the clean-up issue, but also interesting for drug delivery purposes.

^aDipartimento di Scienze Agrarie, Università di Bologna, Viale G. Fanin, 44-40127 Bologna, Italy. E-mail: ilaria.braschi@unibo.it

^bDipartimento di Scienze e Innovazione Tecnologica and Centro Interdisciplinare Nano-SiSTeMI, Università del Piemonte Orientale “A. Avogadro”, Viale T. Michel, 11-15121 Alessandria, Italy. E-mail: maurizio.cossi@mfn.unipmn.it

† Electronic supplementary information (ESI) available. See DOI: 10.1039/c3ra22290j

Table 1 Structures and physico-chemical properties of the sulfonamide antibiotics under investigation

Chemical Structure	Sulfonamides (Acronym)	Molecular weight g mol ⁻¹	pK _a	Water Solubility g L ⁻¹	Adsorption into HSZ-Y ^a % zeolite DW
	Sulfanilamide (SN)	172.2	10.6 ^b	7.50 ^c	3 (n.d.)
	Sulfathiazole (ST)	255.3	7.11 ^d	0.47 ^e	28 (30.2)
	Sulfapyridine (SP)	249.1	8.29 ^b	0.268 ^c	26 (29.0)
	Sulfamerazine (SMZ)	264.3	6.90 ^d	0.202 ^c	28 (29.8)
	Sulfadimethoxine (SDM)	310.3	6.08 ^d	0.345 ^e	28 (29.9)
	Sulfadoxine (SDX)	310.1	5.81 ^f	0.30 ^e	27 (28.9)

^a Data obtained by HPLC analysis (in brackets data obtained by thermogravimetric analysis is reported). pK_a Values are obtained from: ^b ref. 14, ^c ref. 15, ^d ref. 16, ^e ref. 17, ^f ref. 18.

In fact, the reduction of environmental drug pollution can also be achieved by limiting the drug amount released during *in vivo* treatments. The use of matrices for drug delivery usually allows a control of the administered drug amount by increasing its bioavailable portion.

The nature of adsorbed sulfonamides and their arrangement in inorganic matrices can influence their release, and for this reason it is relevant to define the structure of adsorbed species and the interactions involved with the matrix. In the case of sulfadiazine loaded in HSZ-Y, the placement of dimeric species inside zeolite cavities was observed owing to the small dimension of this drug molecule in comparison with the others investigated.¹³

In this study, the embedding into the HSZ-Y was evaluated for six sulfa drugs with different molecular structures and steric hindrances. A combined Fourier transform infrared (FTIR) and solid state nuclear magnetic resonance (SS-NMR) spectroscopy study, augmented with computational model-

ling, allowed us to identify the prevalent tautomer between the amide and imide forms embedded into the HSZ-Y cage for each sulfonamide investigated.

2. Methodologies

A. Materials

Sulfanilamide (4-aminobenzenesulfonamide, SN), sulfathiazole (4-amino-*N*-(1,3-thiazol-2-yl)benzenesulfonamide, ST), sulfamerazine (4-amino-*N*-(4-methylpyrimidin-2-yl)benzenesulfonamide, SMZ), sulfadimethoxine (4-amino-*N*-(2,6-dimethoxy-pyrimidin-4-yl)benzenesulfonamide, SDM), and sulfadoxine (4-amino-*N*-(5,6-dimethoxy-4-pyrimidinyl)benzenesulfonamide, SDX) were purchased as analytical standards from Dr Ehrenstorfer GmbH (Germany) with purities of 99.0%, 99.5%, 99.5%, 97.5%, and 98.0%, respectively. Sulfapyridine (4-amino-*N*-pyridin-2-ylbenzenesulfonamide, SP) was supplied by Fluka Analytical with a purity of 99%. The structure and

physico-chemical properties of the sulfonamides are reported in Table 1.

Y type high silica faujasite zeolite powder with a 200 SiO₂/Al₂O₃ ratio (hereafter named HSZ-Y), 7.0 Å × 7.1 Å access windows and a 12-membered ring window diameter was purchased (code HSZ-390HUA) in its protonated form from Tosoh Corporation (Japan). This zeolite had a total specific surface area of *ca.* 850 m² g⁻¹, most of which was related to the presence of structural micropores (616 m² g⁻¹) as defined elsewhere.¹²

B. Adsorption trials

For each antibiotic 250 mL of 0.3 mM solution was prepared in distilled water and added to 100 mg of HSZ-Y. The amount of antibiotic was calculated in order to slightly exceed the maximum adsorption capacity of HSZ-Y already determined by us for other sulfonamides.¹² According to our study the zeolite adsorption capacity numerically equals the full occupancy of zeolite cavities (*ca.* 4 × 10²⁰ cages per 1 g zeolite) by single antibiotic molecules. The adsorption was conducted at room temperature (RT) in polyallomer centrifuge tubes (Nalgene, New York, USA). Zeolite suspensions were shaken for 2 h and then centrifuged at 20 000 *g* for 15 min. Such a short contact time was chosen because it was already reported that the adsorption of sulfa drugs by HSZ-Y takes a few minutes.¹² Finally, an aliquot of the supernatant was withdrawn and analyzed by HPLC under chromatographic conditions described elsewhere.¹² Under these chromatographic conditions, the retention times for SN, ST, SP, SMZ, SDM, and SDX were 3.08, 3.41, 12.02, 2.71, 5.17, and 5.64 min, respectively. All solvents were HPLC grade.

The loading of antibiotic embedded into HSZ-Y was also confirmed by thermogravimetric analysis (TGA) carried out using experimental conditions already described elsewhere.¹² The TGA results of the sulfa drugs loaded into HSZ-Y are reported in Table 1. The TG and derivative (DTG) profiles are shown in Fig. 1S in the Supporting Information†.

C. Infrared spectroscopy

Fourier transform infrared (FTIR) spectra were collected on a Thermo Electron Corporation FT Nicolet 5700 Spectrometer with 4 cm⁻¹ resolution. Self-supporting pellets of HSZ-Y and HSZ-Y/sulfonamide samples were obtained with a mechanical press at *ca.* 7 tons cm⁻² and placed into an IR cell equipped with KBr windows permanently attached to a vacuum line (residual pressure: ≤1 × 10⁻⁴ Torr; 1 Torr = 133.33 Pa), allowing all treatments and D₂O adsorption experiments to be carried out *in situ*. Air-dried HSZ-Y/sulfonamide samples were outgassed at RT for 30 min in order to remove adsorbed water before FTIR analysis. FTIR spectra of pure sulfonamides in CH₂Cl₂ of spectrophotometric grade (J. T. Baker, NJ, USA) were performed on sulfa drugs in a standard cell for liquids equipped with NaCl windows.

D. Solid state nuclear magnetic resonance spectroscopy

Solid state nuclear magnetic resonance (SS-NMR) spectra were acquired on a Bruker Avance III 500 spectrometer and a wide bore 11.7 Tesla magnet with operational frequencies for ¹H and ¹⁵N of 500.13 and 50.68 MHz, respectively. A 4 mm triple

resonance probe with MAS was employed and the samples were packed on a Zirconia rotor and spun at a MAS rate of 15 kHz. The magnitude of the radio frequency field was 100 kHz for ¹H and the relaxation delay, *d*₁, was between 1 and 600 s. For the ¹⁵N{¹H} CPMAS experiments, the magnetic fields of 100 and 52 kHz were used for initial excitation and decoupling, respectively. During the CP period the ¹H RF field was ramped using 100 increments, whereas the ¹⁵N RF field was maintained at a constant level. During the acquisition, the protons are decoupled from the nitrogen by using a TPPM decoupling scheme. A moderately ramped RF field was used for spin locking, while the nitrogen RF field was matched to obtain an optimal signal and a CP contact time of 2 ms was used. A MAS rate of 5 kHz and a relaxation delay of 1–2 s were employed in all the experiments. All chemical shifts are reported using the δ scale and are externally referenced to TMS at 0 ppm.

E. Models and *ab initio* calculations

All calculations were performed at the density functional level (DFT) with TURBOMOLE V6¹⁹ or Gaussian03 packages.²⁰ The hybrid density functional B3LYP^{21–23} was used, along with a Gaussian-type atomic orbital basis formed by a Hay and Wadt basis set^{24–26} for the Si valence shell, and 6-31G basis set²⁷ supported by polarization functions for all the atoms (resulting in the so-called 6-31G(d,p) set) for all the other elements. Harmonic vibrational spectra were calculated at the same level for the minimum energy conformations: to facilitate the comparison with experimental FTIR spectra, a Gaussian function with 1 cm⁻¹ full width at half maximum (FWHM) was associated to each adsorption line in the simulated spectra.

NMR isotropic chemical shieldings were computed with larger basis sets, namely 6-311+G(d,p)²⁸ and aug-cc-PVTZ²⁹, at the geometries optimized with the above-mentioned smaller basis.

When necessary, the solvent effects on the structures and relative energies were computed using the Conductor-like Polarizable Continuum Model (C-PCM).³⁰

The zeolite cage was extracted from the crystalline structure of faujasite Y (CIF file available as Supplementary Material in ref. 13): the material was formed by tetrahedral cavities approximately 16 Å wide, with four large access windows, formed by 12-membered T rings, while the cavity walls were formed by 4- and 6-membered T rings, each window being shared by two adjacent cavities. In the calculations a single cavity was modeled, using outward pointing -OH to saturate the Si valencies, so that the stoichiometry of the model cage was Si₄₈O₇₂(OH)₄₈. The tridimensional structure of the material, along with a single cavity and the model cavity used in the simulations are shown in Fig. 1 of ref. 13.

During the geometry optimizations, only the adsorbed sulfa drugs were allowed to rearrange, while the zeolite atoms were kept fixed in their crystallographic positions.

3. Results and discussion

Six sulfonamides substituted differently at the sulfonamide nitrogen atom (see the structures in Table 1) were chosen among the most commercialized ones in order to better define the influence of the heterocycle and the nature of its substituents on their confinement in the HSZ-Y cage.

A. Adsorption of sulfa drugs in HSZ-Y

With the exception of sulfanilamide, the amount of the remaining five sulfonamides adsorbed into zeolite was determined by HPLC at 27% zeolite DW on average. A similar figure (28% zeolite DW on average) was found by TG analysis (Table 1). Thermograms are reported in the Supporting Information (Fig. 1S, †). The water content for this hydrophobic zeolite is of *ca.* 1% zeolite weight.¹³ For all antibiotics the maximum weight loss temperatures related to product degradation are different from pure compounds, thus suggesting the embedding of sulfa drug molecules inside zeolite cages. In addition, the loading of sulfa drugs into HSZ-Y is so high that it cannot be explained by a simple adsorption on external zeolite surfaces.

Making a calculation of the maximum adsorption capacity assuming one molecule of sulfonamide per zeolite cage (4×10^{20} cage g^{-1} zeolite DW),¹² the adsorbed amount expected was 17% zeolite DW for sulfathiazole and sulfapyridine, 18% for sulfamerazine, and 21% for sulfadimethoxine and sulfadoxine. The drug amount measured in HSZ-Y upon adsorption is higher than the maximum calculated, thus suggesting the formation of antibiotic multilayers on the external surface of zeolite grains and/or the formation of dimeric species inside zeolite cavities, as already observed for sulfadiazine.¹³

On the contrary, the adsorption of sulfanilamide was limited at about 3% zeolite DW. Sulfonilamide was the first sulfonamide antibiotic to be discovered in 1932¹ and was obtained by the *in situ* hydrolysis of azo dye Prontosil (4-[(2,4-diaminophenyl)azo]benzenesulfonamide). The structure of sulfonilamide is the same as other sulfonamides, except for the presence at the sulfonamide nitrogen of a hydrogen atom in the place of a heterocyclic aromatic ring (Table 1). The scarce adsorption of sulfanilamide may be due to its water solubility, which is exceedingly higher (15–40 times) than the other sulfonamides studied here. Further investigations on the HSZ-Y/sulfanilamide sample were not performed owing to the low affinity of sulfanilamide for hydrophobic HSZ-Y.

The nature of the interactions between sulfa drugs and HSZ-Y was investigated by FTIR, SS-NMR and DFT *ab initio* calculations.

B. Computational modelling

The geometries of the isolated sulfa drugs (except sulfanilamide, *vide supra*) were optimized in vacuum and the harmonic vibrational frequencies were computed at the DFT level to assist the interpretation of FTIR spectra, as discussed below. Different tautomers are possible for such species: we considered the amidic structures, containing the sulfonamide group ($-SO_2-NH-$), along with the imidic forms ($-SO_2=N-$) where the hydrogen atom is bound to a heterocycle nitrogen. The optimized structures of amidic and imidic tautomers of all

considered sulfa drugs are shown in Fig. 1: note that the imidic structures are stabilized by an intramolecular H bond resulting in a 6 membered ring which connects the heterocycle NH to one of the sulfone oxygen atoms. The tautomeric forms involving protonated sulfone oxygen atoms ($-SO(OH)=N-$) were already excluded in a previous work on analogous sulfa drugs, due to their much higher formation energies and the disagreement between calculated and experimental vibrational spectra.¹³

It is known that in the solid state sulfathiazole is more stable in the imidic tautomer, while the amidic form is found in polymorphs I–IV of solid sulfapyridine.³¹ To investigate the tautomer stability of the selected sulfonamides, the optimized energies in vacuum, in dichloromethane and in water were compared using the Gaussian03 package and the C-PCM continuum model for the solvent, with the results reported in Table 2. The calculations indicate that both in vacuum and in solution, the imidic form is favoured only for sulfathiazole, whereas the other sulfa drugs prefer the amidic structure.

Dimers of the same species were also optimized in vacuum, and the corresponding harmonic frequencies computed: in all amidic dimers, two hydrogen bonds establish between the sulfonamide groups and the partner's heterocycle nitrogen atoms. Imidic dimers may even form as discussed below. As suggested by the discussion on the energies calculated for tautomers of isolated sulfa drugs, the dimers also present two distinct minima, with the hydrogen atoms involved in the intermolecular H-bonds closer to sulfonamide or heterocycle nitrogen atoms (dimers formed from amidic or imidic monomers, respectively).

The dimer formation energies are reported in Table 2, referring to the corresponding isolated isomers: note that for sulfathiazole the dimerization energies refer to two monomers in the imide form, while for all the other drugs they refer to amidic monomers. The structure of the most stable sulfa drug dimers are shown in Fig. 1.

As expected, in vacuum the computed formation energies are favourable for all the sulfa drug dimers with respect to the monomers (Table 2). To evaluate the plausibility of dimer formation inside the zeolite cage, sulfathiazole, sulfapyridine, and sulfamerazine dimers were reoptimized in the model cage described above (Fig. 2).

The three dimers remain bound inside the cage, but sulfamerazine is strongly distorted, as indicated by the $N-H \cdots N$ angles (passing from 173° , 174° in vacuum to 154° and 163° in the cage), whereas sulfathiazole and sulfapyridine dimers maintain the planarity of the H-bonded moieties (all the H-bond angles in the cage being in the range 171 – 175°). In general, the optimized structures confirm that sulfathiazole and sulfapyridine dimers are less sterically hindered than sulfamerazine, as is also the case for the other sulfa drugs, bearing even bulkier side groups (see Table 1).

As said above, the harmonic frequencies were computed for all the optimized structures, amidic and imidic monomers and dimers, to have a complete set of theoretical spectra to be compared with the experimental data.

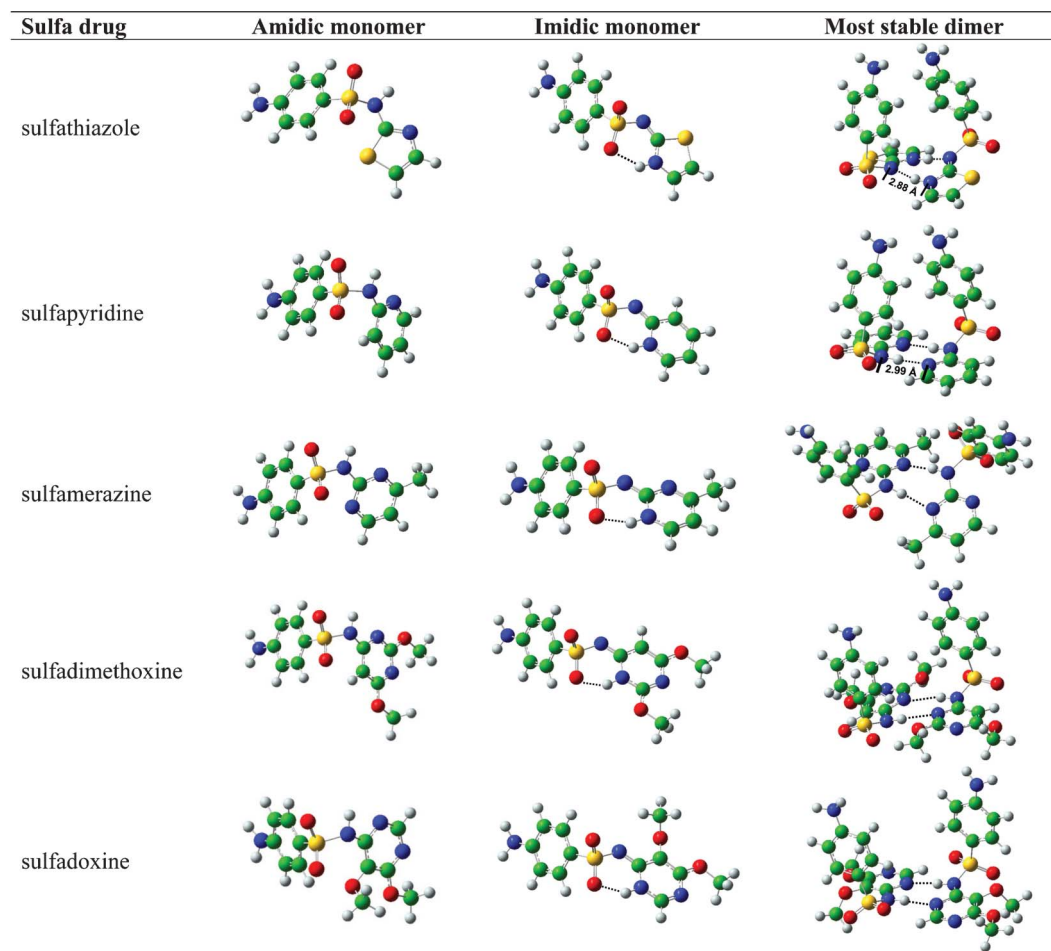
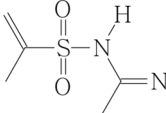
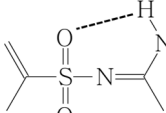
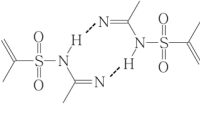
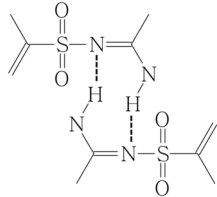


Fig. 1 DFT optimized structure of amidic and cyclic imidic monomers and the most stable dimers of sulfa drugs in vacuum. The imidic form is reported for the sulfathiazole dimer whereas the amidic form is for the other dimers.

Table 2 Computed relative energies (kcal mol⁻¹) of monomeric and dimeric sulfonamide tautomers. For all the drugs, the energies refer to the most stable monomer

Sulfa drug	Medium	Amide monomer	Imide monomer	Amide dimer	Imide dimer
					
Sulfathiazole	vacuum	3.39	0.00	-15.44	-17.07
	CH ₂ Cl ₂	3.49	0.00		
	water	3.48	0.00		
Sulfapyridine	vacuum	0.00	2.18	-17.94	-14.20
	CH ₂ Cl ₂	0.00	1.38		
	water	0.00	1.03		
Sulfamerazine	vacuum	0.00	6.41	-14.04	
	CH ₂ Cl ₂	0.00	3.80		
	water	0.00	3.20		
Sulfadimethoxine	vacuum	0.00	2.40	-13.44	
	CH ₂ Cl ₂	0.00	3.23		
	water	0.00	3.18		
Sulfadoxine	vacuum	0.00	1.95	-11.92	
	CH ₂ Cl ₂	0.00	0.84		
	water	0.00	0.25		

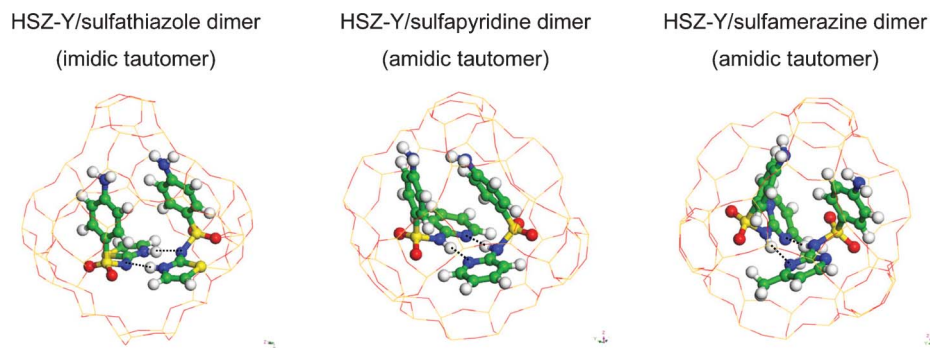


Fig. 2 DFT optimized structure of the most stable tautomers for sulfathiazole, sulfapyridine, and sulfamerazine dimers inside the zeolite Y model cage.

C. Experimental and calculated FT-IR spectra

Calculated bands (FWHM of 1 cm^{-1}) for the amidic tautomers and experimental spectra are reported in Fig. 3.

The computed harmonic frequencies are systematically overestimated, but it can safely be assumed that the spectra pattern is reproduced accurately enough to allow the interpretation, especially when analogous molecules can be compared as in the present case. The visual comparison is helped by downshifting the theoretical frequencies in order to make the first peak for sulfadoxine coincide with the corresponding experimental absorption, and this leads to a shift of 170 and 75 cm^{-1} in the high (Fig. 3A) and in the low frequency region (Fig. 3B), respectively. The main features of the experimental spectra are well reproduced by the calculations, especially in the high wavenumber region where aniline NH_2 and sulfonamide NH stretching vibrations absorb. The most important vibrational frequencies are listed in Table 3 for the five sulfonamides, with the assignments obtained by the comparison of theoretical and experimental results.

For all investigated sulfa drugs, the experimental NH_2 asymmetric (ν_{asym}) and symmetric (ν_{sym}) stretching vibrations

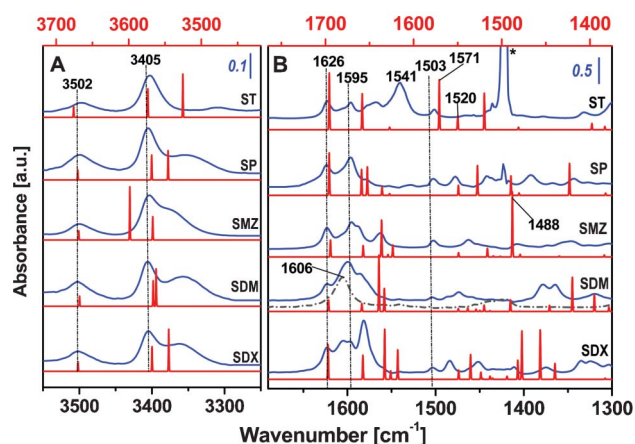


Fig. 3 Infrared spectra of sulfathiazole (ST), sulfapyridine (SP), sulfamerazine (SMZ), sulfadimethoxine (SDM), and sulfadoxine (SDX) in CH_2Cl_2 (blue line) and calculated amidic tautomers *in vacuo* (red line). The IR spectrum of water clusters in CH_2Cl_2 is also reported (black dotted line).

in CH_2Cl_2 are at very similar positions (in the range $3502\text{--}3499$ and $3406\text{--}3402\text{ cm}^{-1}$, respectively), clearly indicating that these vibrational modes are uncoupled from the others arising from the rest of the sulfonamide structure. The corresponding harmonic vibrations in the calculated spectra are at $3676\text{--}3668$ and $3574\text{--}3566\text{ cm}^{-1}$, respectively. These modes are found at positions similar to those reported in the literature for other sulfa drugs.¹³

The stretching frequency of the sulfonamide NH group significantly differs among the five antibiotics, falling in the range $3375\text{--}3307\text{ cm}^{-1}$ and following the order: sulfamerazine $>$ sulfadoxine \geq sulfapyridine \geq sulfadimethoxine \gg sulfathiazole. This trend, conversely to what has been reported for other sulfa drugs,¹³ does not follow the acidic character of the sulfonamide group of the compounds here investigated ($\text{p}K_{\text{a}}$, Table 1). Experimentally, sulfathiazole ($\text{p}K_{\text{a}}$ 7.11) presents the lowest amide NH stretching frequency (3307 cm^{-1}) whereas sulfamerazine ($\text{p}K_{\text{a}}$ 6.90) shows the highest value at 3375 cm^{-1} . The computed harmonic frequencies do not follow the acidity of the antibiotics as well, and the trend roughly resembles what was experimentally found: NH stretching at the lowest wavenumbers (3525 cm^{-1}) for sulfathiazole and at the highest frequency (3598 cm^{-1}) for sulfamerazine.

The discrepancy between acidic constants and sulfonamidic NH stretching frequencies can be explained considering that: i) the $\text{p}K_{\text{a}}$ values were determined in a polar solvent like water, whereas the IR spectra were collected in a nonpolar solvent like CH_2Cl_2 ; ii) the sulfonamide NH vibration depends on the molecular and electronic structure of the molecule as a whole, whereas the $\text{p}K_{\text{a}}$ is influenced by the solvating effects of water on both neutral and anionic forms of the sulfa drug.

As far as the intensity of the NH stretching absorption is concerned, the sulfathiazole band is significantly the least pronounced among the five sulfonamides. This feature suggests that the occurrence of both the amidic and imidic monomers for sulfathiazole (see calculated NH stretching at 3525 and 3473 cm^{-1} , Fig. 4A, curves c and d, respectively) are limited and that the dimeric species should be present as indicated by the experimental broad band in the region $3200\text{--}2500\text{ cm}^{-1}$ (see below, Fig. 4–6, for a detailed assignment of this band). On the contrary, the higher NH stretching intensity of the other sulfa drugs strongly suggests that sulfapyridine,

Table 3 Infrared wavenumbers (cm^{-1}) for the amidic form of sulfonamides computed *in vacuo* and experimentally obtained in CH_2Cl_2 and after adsorption into the HSZ-Y zeolite

Vibrational modes	Sulfathiazole		Sulfapyridine		Sulfamerazine		Sulfadimethoxine		Sulfadoxine	
	In	Adsorbed	In	Adsorbed	In	Adsorbed	In	Adsorbed	In	Adsorbed
	CH_2Cl_2	in HSZ-Y ^a	CH_2Cl_2	in HSZ-Y ^a	CH_2Cl_2	in HSZ-Y ^a	CH_2Cl_2	in HSZ-Y ^a	CH_2Cl_2	in HSZ-Y ^a
$\nu_{\text{asym}}\text{NH}_2$	3500	3487	3670	3499	3669	3490	3668	3502	3502	3502
$\nu_{\text{sym}}\text{NH}_2$	3402	3392	3568	3406	3567	3404	3566	3405	3405	3405
ν_{NH}	3307	3200–2700	3546	3358	3598	3375	3562	3357	3383 (sh)	3362
$2\delta\text{NH}_2$		3240		3246		3244		3248		3248
δNH_2	1696	1628	1696	1624	1694	1626	1696	1623	1697	1626
$\nu_{\text{Ph}} \text{quadrant} + \delta\text{NH}_2$	1658	1597	1659	1598	1657	1597	1659	1599	1657	1595
$\nu_{\text{het}} \text{C}-\text{C} + \nu_{\text{het}} \text{C}-\text{N}$		1597 (sh)		1597		1595		1597		1595
$\nu_{\text{het}} \text{C}-\text{C} + \nu_{\text{het}} \text{C}-\text{N} + \delta\text{NH}$	1571	n.d.	1633	1580	1636	1588 (sh)	1633	1586 (sh)	1633	1581
	1520		1634			1562			1605	—
$\nu_{\text{het}} \text{vibr} + \delta\text{NH}$			1527	1477						
$\delta\text{Ph in-plane CH}$			1490	1443						
$\nu_{\text{amide}} \text{N-het C} + \text{het vibr} + \delta\text{CH}_3$	1550	1502	1549	1503	1549	1503	1549	1504	1549	1503
$\delta\text{NH in-plane}$	1519		1490		1488		1490		1477	1452
	1398		1423	1393					1440	1450

^a Frequencies attributed to the dimeric species.

sulfamerazine, sulfamethazine, and sulfadoxine are present in amidic form (Fig. 3A).

The experimental spectra of sulfonamides in CH_2Cl_2 show complex bands in the $1640\text{--}1500 \text{ cm}^{-1}$ region (Fig. 3B), where vibrations of NH_2 bending along with phenyl and aromatic heterocycle stretchings, which are often coupled with each other, occur. For this reason a detailed description of specific contributions is difficult, though some absorptions are clearly assignable. As expected, the amino in-plane bending mode (δNH_2) for the five sulfa drugs is found at a very similar frequency in the $1626\text{--}1620 \text{ cm}^{-1}$ range and is well reproduced by the computational model ($1697\text{--}1694 \text{ cm}^{-1}$). Bands at $1599\text{--}1595 \text{ cm}^{-1}$ are assigned to phenyl quadrant stretching coupled to NH_2 bending (the corresponding computed spectra show bands in the range $1659\text{--}1657 \text{ cm}^{-1}$). This mode is well defined in all sulfonamide spectra, with the exception of sulfamerazine and sulfadoxine where it is overlapped to an intense contribution at 1606 cm^{-1} , due to water (see dotted curve in Fig. 3B) present in these sulfa drugs formulations.

As far as the heterocycle vibrations are concerned, two main vibrational modes of the heterocyclic ring, due to the C–C and the C–N bonds stretchings, are predicted by the DFT calculation and some of them are found to be coupled with the sulfonamide NH bending (see Table 3 for details). Another vibrational mode that does not change significantly among the five sulfa drugs is the phenyl in-plane bending at $1504\text{--}1502 \text{ cm}^{-1}$ in the experimental spectra and in the $1550\text{--}1549 \text{ cm}^{-1}$ range in the calculated ones.

The experimental spectrum for sulfathiazole significantly differs from that of the calculated spectrum in the amidic form: only for this drug a strong experimental absorption at 1541 cm^{-1} is present. In addition, specific vibrations for the sulfathiazole heterocycle, coupled with NH_2 bending, calculated at 1571 and 1520 cm^{-1} , are not evident in the experimental spectrum (only weak and broad bands are found in the $1480\text{--}1450 \text{ cm}^{-1}$ range), therefore strengthening the

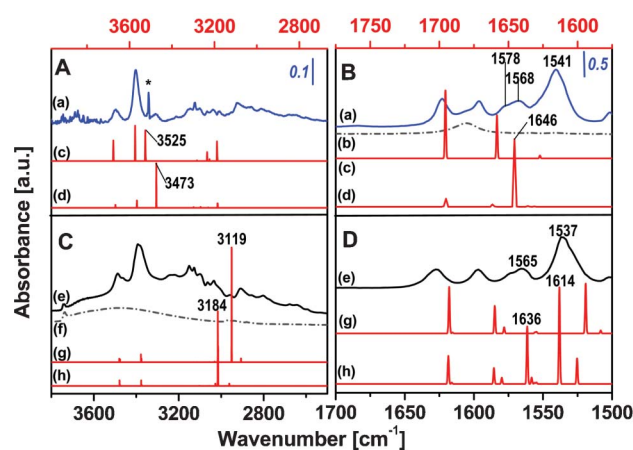


Fig. 4 Experimental infrared spectra of sulfathiazole in CH_2Cl_2 (curve a) and adsorbed into zeolite HSZ-Y (curve e). The experimental spectra of water in CH_2Cl_2 (curve b) and bare HSZ-Y (curve f) are also reported. The calculated spectra of amide and imide monomers (curves c and d, respectively) and amide and imide dimers (curves g and h, respectively) are reported for comparison. Asterisk indicates unreliable band due to solvent subtraction.

hypothesis that the sulfathiazole amidic form poorly contributes to the experimental features.

In Fig. 4, the computed spectra of the amidic and imidic monomers and dimers of sulfathiazole in vacuum are compared to the experimental spectrum of sulfathiazole in CH_2Cl_2 , especially enlightening the region at $1650\text{--}1500\text{ cm}^{-1}$.

The computed spectrum of imidic tautomer (curve d) shows an intense band at 1646 cm^{-1} due to an imide NH bending mode, which can be observed in the experimental spectrum (curve a) at 1578 cm^{-1} . The strong absorption at 1541 cm^{-1} (curve a) is absent in both the computed amidic and imidic monomer spectra (curves c and d, respectively). For an assignment of this contribution, a study of the spectroscopic features of the dimeric species is necessary. Computed spectra of amidic and imidic dimers are reported in Fig. 4D (curves g and h): only in the case of the imidic dimer two strong absorptions are calculated at 1636 and 1614 cm^{-1} (curve h) due to two modes of NH bending coupled to ring modes. These modes are clearly identified in the experimental spectrum at 1568 and 1541 cm^{-1} , thus indicating that the imide dimer is the most abundant sulfathiazole species in CH_2Cl_2 . The formation of this species in a very diluted nonpolar solvent, such as dichloromethane, is not surprising in that, according to the stabilization energy computed in vacuum (Table 2), dimers of sulfathiazole in the imidic form are the most stable.

All these results lead to the evidence of the occurrence of a consistent contribution of the imidic dimer species for sulfathiazole in CH_2Cl_2 , whereas for the other sulfonamides investigated the more stable amidic form is identified.

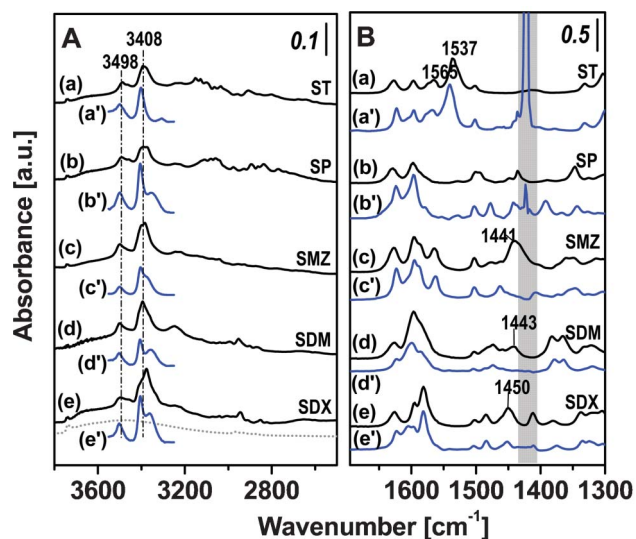


Fig. 5 Infrared spectra of sulfathiazole (ST), sulfapyridine (SP), sulfamerazine (SMZ), sulfadimethoxine (SDM), and sulfadoxine (SDX) adsorbed into HSZ-Y (black lines a–e). The spectra of sulfonamides in CH_2Cl_2 (blue lines a'–e') are reported for comparison. The spectrum of pure HSZ-Y is shown by the dotted line. The highlighted gray region in the spectra in CH_2Cl_2 shows some artefacts due to the solvent subtraction.

D. Sulfonamides adsorbed in HSZ-Y

As far as the adsorption of sulfonamides into zeolite is concerned, it is interesting to note that the position of the NH_2 stretching bands ($3500\text{--}3487\text{ cm}^{-1}$ and $3389\text{--}3411\text{ cm}^{-1}$) is almost unchanged for the molecules embedded within the zeolite cages (Fig. 5A, Table 3). However, each band is split into a number of overlapping components. This feature is characteristic of molecules experiencing slightly different environments, either in the cage or on the external surfaces of the zeolite crystallites.

The sulfonamide NH stretching of sulfamerazine, sulfadimethoxine and sulfadoxine is only weakly perturbed upon adsorption into zeolite: this band slightly moves to higher frequencies overlapping the band of symmetrical NH_2 stretching, and for this reason it is difficult to define a precise position. These small variations are due to very weak interactions with oxygen atoms of the cage wall. On the contrary, the NH stretching of sulfathiazole and sulfapyridine in the adsorbed phase moves to frequencies ranging between $3200\text{--}2700\text{ cm}^{-1}$ (also where CH stretching vibrations of phenyl and heterocyclic rings absorb), indicating the formation of H-bonds.

The position of the H-bonded sulfonamide NH band cannot be measured with precision because it falls in a region where Fermi resonance interactions with overtones and/or combination bands of the sulfa drugs occur, and this leads to several maxima overlapped with the broad $\text{NH}\cdots\text{N}$ absorption. A similar broad band has been found in a recent study in sulfadiazine sulfonamide adsorbed in the same HSZ-Y used in this study.¹³ In adsorbed sulfadiazine, a NH stretching downward shift of about 250 cm^{-1} was attributed to the formation of dimeric species inside the zeolite cage where the sulfonamide group is H-bonded to the heterocycle nitrogen ($\text{NH}\cdots\text{N}$) of another sulfadiazine molecule. H-bonded dimers can also form in the case of sulfathiazole and sulfapyridine

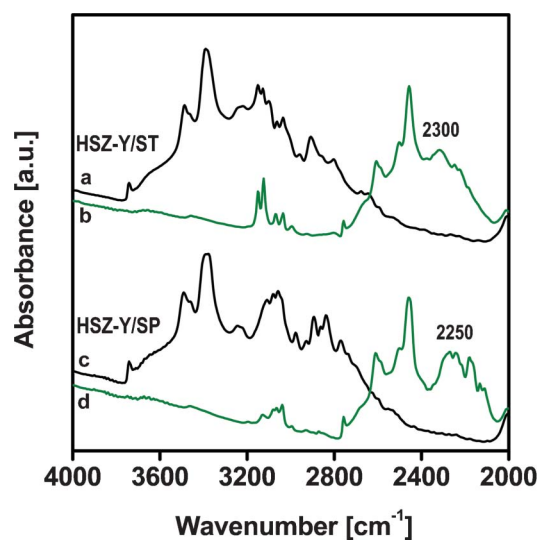


Fig. 6 Infrared spectra of sulfathiazole (ST) and sulfapyridine (SP) adsorbed into HSZ-Y zeolite before (black curves a and c) and after treatment with D_2O (green curves b and d).

because of the favourable position of their heterocycle nitrogen atoms described above in the computational modeling.

In this study the presence of a large band for H-bonded NH stretching in the 3200–2700 cm^{-1} range was confirmed by deuteration of sulfathiazole and sulfapyridine (Fig. 6).

Upon deuteration the NH_2 and NH stretching absorptions are downward shifted in the 2800–2000 cm^{-1} range, except the CH stretching vibrations of the phenyl and heterocyclic rings, which become more clearly visible in the 3200–3000 cm^{-1} range. It is evident that the deuterated spectra (curves b and d) are simplified especially in the 2400–2050 cm^{-1} region where $\text{ND}\cdots\text{N}$ species absorb, and this is because the Fermi resonance effects are strongly depleted. The position of the maxima is more clearly determined at around 2300 and 2250 cm^{-1} , respectively, for sulfathiazole and sulfapyridine. We can thus safely assume that the position of the $\text{NH}\cdots\text{N}$ bands (curves a and c) follows the same order, being at higher wavenumbers for sulfathiazole than sulfapyridine. This experiment definitely confirms that sulfathiazole and sulfapyridine dimers are formed in the HSZ-Y cage upon adsorption.

As far as the vibrational modes in the 1700–1500 cm^{-1} region are concerned (Fig. 5B), only small changes are evident by comparing sulfonamides adsorbed into the zeolite and in CH_2Cl_2 solution.

In the 1500–1400 cm^{-1} spectral region, a noticeable difference in the spectrum of sulfamerazine (SMZ) in the adsorbed phase is the presence of a broad and intense band at 1441 cm^{-1} . In this region the computed spectrum shows an intense vibration at 1488 cm^{-1} due to the heterocycle carbon-amide nitrogen stretching. The reason why this band is more evident in the spectrum of the adsorbed sulfamerazine than in CH_2Cl_2 is not clear, however, it is reasonable to assume that the intensity of this mode is related to the interaction of the heterocycle with the cage wall. The stretching of the C–N bond connecting the heterocycle to the sulfonamide group is found at 1443 and 1450 cm^{-1} in the case of sulfadimethoxine and sulfadoxine, respectively, adsorbed into zeolite. Likely, the heterocycle of these drugs experiences similar environments upon adsorption. The mode at 1441–1450 cm^{-1} is not active in sulfapyridine adsorbed into zeolite in the dimeric form because of the $\text{NH}\cdots\text{N}$ intermolecular hydrogen bonding.

The case of sulfathiazole needs to be specifically discussed in that this is the only sulfa drug present in imidic forms (monomer and dimer) in CH_2Cl_2 solution. Upon adsorption, the sulfathiazole spectrum in the low frequency region (Fig. 5B) is similar to that in CH_2Cl_2 and the absorptions at 1565 and 1537 cm^{-1} , assigned to two NH bending modes of imide dimers are clearly detected. This effect is more clearly presented in Fig. 4B and 4D, where the experimental spectra (curves a and e for sulfathiazole in CH_2Cl_2 and adsorbed into HSZ-Y, respectively) are compared to the calculated monomers and dimers in both amidic and imidic form. Two asymmetric (3648 and 3644 cm^{-1}) and two symmetric stretching modes (3546 and 3543 cm^{-1}) computed for the NH_2 of the amidic sulfathiazole dimer (curve g) are found, whereas for the imidic dimers (curve h) they are calculated at 3647, 3644, 3545, and 3543, respectively. As far as the NH stretching modes of the dimer are concerned, the asymmetric and symmetric NH

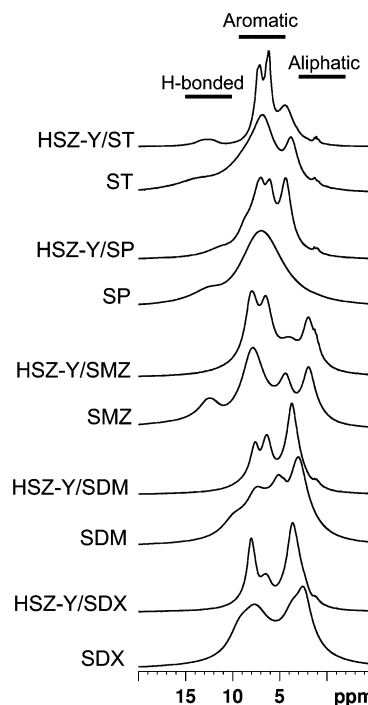


Fig. 7 ^1H NMR spectra of sulfathiazole (ST), sulfapyridine (SP), sulfamerazine (SMZ), sulfadimethoxine (SDM), and sulfadoxine (SDX) adsorbed into HSZ-Y zeolite. Spectra of pure antibiotics are reported for comparison.

absorptions were calculated at 3119 and 3075 cm^{-1} (weak) and at 3184 and 3130 cm^{-1} (very weak) for the amidic and imidic tautomer, respectively. As discussed above, this region cannot be used to distinguish one dimer tautomer from the other because of the very similar corresponding frequencies.

It is worth recalling, the calculated spectrum of the imidic dimer (Fig. 4D, curve h) shows two strong bands at 1636 and 1614 cm^{-1} due to the two modes of imidic NH bending, which definitely explains the presence of the strong absorption at 1568 and 1537 cm^{-1} in the experimental spectrum (curve e) of sulfathiazole adsorbed into HSZ-Y.

E. Solid state NMR spectroscopy

A SS-NMR study was used to support the IR findings on the nature of the sulfa drug tautomers in the adsorbed phase. In addition, theoretical chemical shieldings were computed for all the drugs, both monomers and dimers: the full list of ^1H , ^{13}C and ^{15}N chemical shifts (referred to NH_3 and TMS at the same level) is available as Supplementary Material.† The most relevant computational results are discussed below.

Fig. 7 shows the ^1H MAS NMR spectra recorded at a moderate MAS rate (15 kHz) on different sulfa drugs adsorbed on zeolite. For the purpose of comparison, the ^1H MAS NMR spectra of solid crystalline sulfa drugs are also presented.

Very broad peaks of the crystalline sulfa drugs are due to the non-averaging of $^1\text{H}-^1\text{H}$ homonuclear dipolar couplings, nevertheless, a moderate MAS rate is sufficient to resolve the highly polarized H-bonded proton chemical shifts.³² While in sulfathiazole and sulfapyridine the chemical shifts due to H-bonded protons are visible as weak and broad signals in the

range 14.0–13.0 ppm, a well resolved peak at 12.5 ppm is seen in sulfamerazine. Such low-field proton chemical shifts indicate strong H-bonding in the crystalline state and are absent in pure sulfadimethoxine and sulfadoxine.

In the adsorbed samples, the ^1H MAS spectra are dominated by aliphatic and aromatic proton peaks in sulfamerazine (HSZ-Y/SMZ), sulfadimethoxine (HSZ-Y/SDM) and sulfadoxine (HSZ-Y/SDX), whereas only aromatic peaks in sulfathiazole (HSZ-Y/ST) and sulfapyridine (HSZ-Y/SP) were detected. Clearly, the existence of H-bonded proton sites are only visible in two adsorbed systems, namely, HSZ-Y/ST (12.2, 13.3 ppm) and HSZ-Y/SP (11.0 ppm). Noncovalent interactions (mainly H-bonding, van der Waals and hydrophilic/hydrophobic interactions) play a fundamental role in the adsorption of sulfa drugs in HSZ-Y due to their selectivity, specificity, directionality and strength.¹³ All the sulfa drugs under study are capable of forming intermolecular hydrogen bonding of the nature $\text{N-H}\cdots\text{O}$ and $\text{N-H}\cdots\text{N}$. However, only HSZ-Y/ST and HSZ-Y/SP show strong H-bonding as evident from the low-field peaks in full agreement with the formation of dimers shown by the computational modelling and IR combined study. The computed chemical shifts (see Supplementary Material †) agree with this picture: in all the dimers the protons involved in the intermolecular H-bond are markedly shifted downfield with respect to the monomers, moving e. g. from 10.4 to 14.2 ppm for ST, and from 6.2 to 12.7 for SP.

As discussed for HSZ-Y/ST, two low-field peaks (12.2, 13.3 ppm) corresponding to the two distinct H-bonded protons can be observed, however, in HSZ-Y/SP, only one broad low-field peak (11.0 ppm) is found. It is further interesting to note that, low-field peaks were observed for pure sulfathiazole (ST: 14.0 ppm) and sulfapyridine (SP: 13.0 ppm) with a marked increase in the isotropic chemical shifts compared to loaded zeolite systems. Such pronounced differences in the chemical shifts indicate a more disordered packing arrangement in adsorbed systems as compared to pure crystalline drugs. In general, three dimensionally extending intermolecular and intramolecular H-bonding links between dimers forming chains, ladders, layers, *etc.* are observed in pure crystalline sulfa drugs,³³ however, such extended structure formation is impossible in the adsorbed systems due to the space restriction of cages. The difference in the H-bonded resonances in HSZ-Y/ST and HSZ-Y/SP could be explained in terms of the interplay between the changing electronic and steric effects of the thiazole/pyridine ring.

Focusing on the remaining adsorbed systems, the absence of dimer formation in HSZ-H/SMZ, HSZ-Y/SDM and HSZ-Y/SDX can be rationalized in terms of the increased steric effects on the heterocyclic ring due to the methyl/methoxyl substitution. With increasing heterocycle substitution, the steric bulk of the methyl/methoxyl groups hinders the approach of the monomers to form intermolecular H-bonded dimer links.

The molecular nature of the sulfa drugs in HSZ-Y was determined by $^{15}\text{N}\{^1\text{H}\}$ CPMAS NMR experiments in ^{15}N natural abundance. Fig. 8 shows the ^{15}N CPMAS spectra of sulfa drugs adsorbed into HSZ-Y which are recorded at RT with a short contact time (2 ms) and a moderate MAS rate (5 kHz).

All the spectra show 2 resonances due to the NH_2 and NH at around 62 ppm and 140 ppm (reference solid: glycine, 32.9

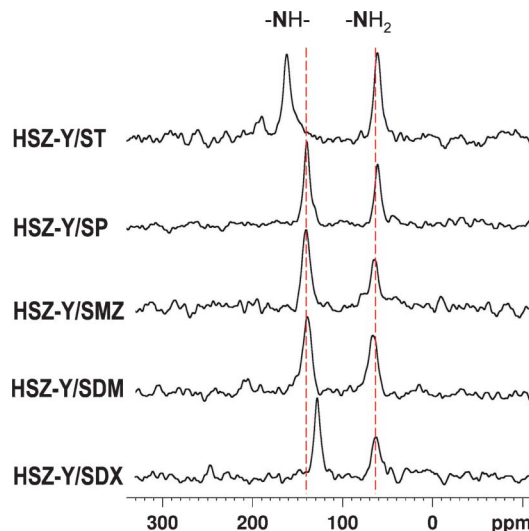


Fig. 8 $^{15}\text{N}\{^1\text{H}\}$ CPMAS NMR spectra of HSZ-Y zeolites adsorbed sulfathiazole (HSZ-Y/ST), sulfapyridine (HSZ-Y/SP), sulfamerazine (HSZ-Y/SMZ), sulfadimethoxine (HSZ-Y/SDM) and sulfadoxine (HSZ-Y/SDX).

ppm), respectively, except for the HSZ-Y/ST. In contrast to the expectations of a single band for NH in HSZ-Y/ST, two peaks at 162 and 190 ppm were observed. All the resonances are expected from the protonated ^{15}N as a short cross polarization contact time was used in all experiments. The dramatic low field shift and the existence of two different resonances for the NH group can be due to different geometries around this nitrogen which are fixed by the molecular environment. The absence of a unique intrinsic chemical shift for the same NH group was assumed to be due to the proton disorder at ^{15}N . In other words, either two different NH groups, which interconvert rapidly, or more tautomers are expected.

The comparison with theoretical chemical shifts (see Supplementary Material †) can help to analyze the results: note that the calculations refer to isolated drugs (either monomers or dimers) and thus a systematic error with respect to the adsorbed samples is expected, nonetheless the shape of the spectra can be fruitfully compared. The computed chemical shifts for NH_2 occur at similar values for all the monomer systems, and little variations are found when passing to dimers. The lower field resonances are attributed to the heterocycle NH group in imidic ST and to the $\text{SO}_2\text{-NH}$ moiety in the other drugs: notably, ST is the only system which exhibits a marked downfield shift passing from monomer to dimer (163 to 184 ppm). One can see that the experimental NMR spectra are not compatible with the presence of monomer ST (which would be expected to show a lower chemical shift than all the other systems), while they qualitatively agree with the presence of dimer ST (for which a higher chemical shift is computed). ^{15}N spectra provide little information about dimer SP species, since their resonance is computed in the same range as for monomer drugs: on the other hand, the ^1H spectra commented on above clearly show the presence of H-bonding also in this system, unlike SMZ, SDM and SDX.

4. Conclusions

In the present study the occurrence of monomeric and dimeric species of sulfonamide antibiotics inside high silica zeolite Y (HSZ-Y) cage was studied by loading sulfa drugs of different dimensions and nature of substituents from water solutions. The adsorption of five out of the six sulfa drugs by HSZ-Y is remarkable, attesting at around 28% zeolite DW on average, being interesting for both the purpose of water depollution and drug delivery issues. The drug solubility negatively affected the adsorption as shown by the scarce loading of highly soluble sulfanilamide.

The host-guest and guest-guest interactions of the zeolite-drug and drug-drug complexes have been studied by FT-IR, SS-NMR and computational modeling. Sulfonamides of the lowest dimensions (sulfathiazole and sulfapyridine) were able to form dimers inside the zeolite cage, whereas those of the biggest size (sulfamerazine, sulfadimethoxine, and sulfadoxine) were embedded as single molecules.

The ability of sulfonamides to exist under amidic or imidic tautomeric forms has been known for many decades, but the involved studies dealt with crystal structures. In this study, the most stable tautomer of sulfonamides in dichloromethane and embedded into a zeolite cage was defined and, for the first time, $^{15}\text{N}\{^1\text{H}\}$ CPMAS NMR spectroscopy was successfully used to confirm the most stable tautomer of the sulfa drugs embedded into the inorganic matrix. Due to the favourable stabilization energy, both monomers and dimers of imide sulfathiazole and amidic sulfapyridine were embedded inside a zeolite cage, whereas the other sulfa drugs were adsorbed as single molecules in amidic form.

Acknowledgements

Research co-funded by the Italian Ministry of Education, University, and Research (Project “Zeolites as nano-reactors for the environment: efficiency, selectivity and stability in the adsorption of drugs from contaminated waters”; DM n. 1407 del 4 Dicembre 2008). G. G. and G. P. acknowledge Regione Piemonte for a post-doc fellowship. The financial support from “Fondazione Compagnia di San Paolo” for the acquisition of Bruker Avance III 500 SS-NMR spectrometer is gratefully acknowledged. Dr Daniela Montecchio is acknowledged for TG analysis.

References

- 1 G. Domagk, *Dtsch. Med. Wochenschr.*, 1935, **61**, 250.
- 2 B. A. Hemstreet, *Pharmacotherapy*, 2006, **26**, 551.
- 3 A. K. Sarmah, M. T. Meyer and A. B. Boxall, *Chemosphere*, 2006, **65**, 725.
- 4 W. Reybroeck, *Apiacta*, 2003, **38**, 23.
- 5 A. Gentili, D. Perret, S. Marchese, M. Sergi, C. Olmi and R. Curini, *J. Agric. Food Chem.*, 2004, **52**, 4614.
- 6 Z. Qiang and C. Adams, *Water Res.*, 2004, **38**, 2874.
- 7 A. B. A. Boxall, P. Blackwell, R. Cavallo and P. Kay Tolls, *Toxicol. Lett.*, 2002, **131**, 19.
- 8 G. Hamscher, H. Pawelzick, H. Höper and H. Nau, *Environ. Toxicol. Chem.*, 2005, **24**, 861.
- 9 J. Acar and B. Rostel, *Rev. Sci. Tech.*, 2001, **20**, 797.
- 10 F. C. Cabello, *Environ. Microbiol.*, 2006, **8**, 1137.
- 11 A. Rossner, S. A. Snyder and D. R. U. Knappe, *Water Res.*, 2009, **43**, 3787.
- 12 I. Braschi, S. Blasioli, L. Gigli, C. E. Gessa, A. Alberti and A. Martucci, *J. Hazard. Mater.*, 2010, **178**, 218.
- 13 I. Braschi, G. Gatti, G. Paul, C. E. Gessa, M. Cossi and L. Marchese, *Langmuir*, 2010, **26**, 9524.
- 14 R. F. Cross and J. Cao, *J. Chromatogr., A*, 1998, **818**, 217.
- 15 Z. Qiang and C. Adams, *Water Res.*, 2004, **38**, 2874.
- 16 L. Geiser, Y. Henchoz, A. Galland, P.-A. Carrupt and J.-L. Veuthey, *J. Sep. Sci.*, 2005, **28**, 2374.
- 17 <http://www.drugbank.ca>.
- 18 M. Kanke and K. Sekiguchi, *Chem. Pharm. Bull.*, 1973, **21**, 878.
- 19 R. Ahlrichs, M. Bar, M. Haser, H. Horn and C. Kolmel, *Chem. Phys. Lett.*, 1989, **162**, 165.
- 20 M. J. Frisch, G. W. Trucks and H. B. Schlegel, *et al.*, *Gaussian03, release C.02*, Gaussian Inc. Wallingford CT, 2004.
- 21 A. D. Becke, *Phys. Rev. A: At., Mol., Opt. Phys.*, 1988, **38**, 3098.
- 22 C. Lee, W. Yang and R. G. Parr, *Phys. Rev. B*, 1988, **37**, 785.
- 23 A. D. Becke, *J. Chem. Phys.*, 1993, **98**, 5648.
- 24 P. J. Hay and W. R. Wadt, *J. Chem. Phys.*, 1985, **82**, 270.
- 25 W. R. Wadt and P. J. Hay, *J. Chem. Phys.*, 1985, **82**, 284.
- 26 P. J. Hay and W. R. Wadt, *J. Chem. Phys.*, 1985, **82**, 299.
- 27 P. C. Hariharan and J. A. Pople, *Theor. Chim. Acta*, 1973, **28**, 213.
- 28 A. D. McLean and G. S. Chandler, *J. Chem. Phys.*, 1980, **72**, 5639.
- 29 R. A. Kendall, T. H. Dunning Jr. and R. J. Harrison, *J. Chem. Phys.*, 1992, **96**, 6796.
- 30 V. Barone and M. Cossi, *J. Phys. Chem. A*, 1998, **102**, 1995.
- 31 S. E. Lawrence, M. T. McAuliffe and M. A. Moynihan, *Eur. J. Org. Chem.*, 2010, **6**, 1134.
- 32 V. E. Zorin, S. P. Brown and P. Hodgkinson, *J. Chem. Phys.*, 2006, **125**, 144508.
- 33 D. A. Adsmo and D. J. W. Grant, *J. Pharm. Sci.*, 2001, **90**, 2058.